

A Noise-Resistant Superpixel Segmentation Algorithm for Hyperspectral Images

Peng Fu^{1,2}, Qianqian Xu¹, Jieyu Zhang³ and Leilei Geng^{4,*}

Abstract: The superpixel segmentation has been widely applied in many computer vision and image process applications. In recent years, amount of superpixel segmentation algorithms have been proposed. However, most of the current algorithms are designed for natural images with little noise corrupted. In order to apply the superpixel algorithms to hyperspectral images which are always seriously polluted by noise, we propose a noise-resistant superpixel segmentation (NRSS) algorithm in this paper. In the proposed NRSS, the spectral signatures are first transformed into frequency domain to enhance the noise robustness; then the two widely spectral similarity measures-spectral angle mapper (SAM) and spectral information divergence (SID) are combined to enhance the discriminability of the spectral similarity; finally, the superpixels are generated with the proposed frequency-based spectral similarity. Both qualitative and quantitative experimental results demonstrate the effectiveness of the proposed superpixel segmentation algorithm when dealing with hyperspectral images with various noise levels. Moreover, the proposed NRSS is compared with the most widely used superpixel segmentation algorithm-simple linear iterative clustering (SLIC), where the comparison results prove the superiority of the proposed superpixel segmentation algorithm.

Keywords: Superpixel segmentation, hyperspectral images, fourier transformation, spectral similarity, random noise.

1 Introduction

In recent years, superpixel segmentation has been widely used as a preprocessing step of various computer vision applications, such as image segmentation [Frag, Lu, Roth et al. (2017)], saliency detection [Liu, Li, Ye et al. (2017)], target tracking [Wang, Wang, Liu et al. (2018)], image classification [Zhang, Zheng and Xia (2018)], and so on. In general, the existing superpixel segmentation algorithms can be categorized as graph-based or gradient-

¹ School of Computer Science and Engineering, Nanjing University of Science and Technology, Nanjing, 210094, China.

² School of Information Technologies, The University of Sydney, Sydney, NSW2006, Australia.

³ School of Science, China Pharmaceutical University, Nanjing, 211198, China.

⁴ Institute of Computer Science and Technology, Shandong University of Finance and Economics, Jinan, 250014, China.

* Corresponding Author: Leilei Geng. Email: leileigeng_njust@163.com.

based approaches. The classical graph-based algorithms include the Normalized cuts algorithm [Shi and Malik (2000)], the superpixel lattice algorithm [Moore, Prince, Warrell et al. (2008)], the Entropy rate superpixel segmentation [Liu, Tuzel, Ramalingam et al. (2011)]. Typical graph-based algorithms include Watersheds algorithm [Vincent and Soille (1991)], Quick-shift algorithm [Vedaldi and Soatto (2018)], Turbopixel algorithm [Levinshtein, Stere, Kutulakos et al. (2009)]. In recent years, the clustering techniques [He, Ouyang, Wang et al. (2018)] have been widely used in the superpixel segmentation algorithms, where the simple linear iterative clustering (SLIC) [Achanta, Shaji, Smith et al. (2012)] is the most prominent one. The detailed descriptions and performance comparison of these superpixel segmentation algorithms can be found in [Wei, Yang, Gong et al. (2018)]. The most desirable property of a superpixel segmentation algorithm is that the generated superpixels should be tightly adhering to the image boundaries. In general, the current superpixel segmentation algorithms are designed for natural images, where the noise is very limited in these images. However, the hyperspectral (HS) images are more likely to be corrupted by random noise due to the weak energy acquired in each spectral band. In practice, when we apply the existing algorithms to segment a HS image into superpixels, the generated superpixels are always affected by the noise. To address this challenge, we propose a novel noise-resistant superpixel segmentation (NRSS) algorithm for the noisy HS images in this paper. In order to make the superpixel algorithm more robust to noise, a new spectral similarity measure is designed in frequency domain. Experimental results show the effectiveness and superiority of the proposed NRSS algorithm.

2 Noise-resistant superpixel segmentation algorithm

Given a HS image with the size $X \times Y \times N$, where X and Y represent the length and width of the spatial image, and N is the total number of the spectral bands. First, the spatial image within one band is divided into K blocks with block size equals S . Then, an initial cluster center can be defined as follows:

$$\mathbf{R}_k = [x_k \ y_k \ \boldsymbol{\psi}_k] \quad (1)$$

in which \mathbf{R}_k represents the initial center; x_k and y_k are the spatial coordinates; $\boldsymbol{\psi}_k$ denotes the vector of spectral signatures of the center. After the initialization step, we assign each pixel to the closest center by using a new similarity measure, where the proposed measure is composed of a spatial similarity term and a spectral similarity term. In order to enhance the noise robustness of the algorithm, the spectral similarity is defined in frequency domain. In the proposed NRSS algorithm, we adopt the discrete Fourier transform (DFT) to transform the spectral information into frequency domain, which can be formulated as:

$$F(u) = \sum_{n=0}^{N-1} f(n) e^{-\tau \frac{2\pi}{N} nu}, \quad \tau = \sqrt{-1} \quad (2)$$

in which u denotes the frequency; N is the total number of the spectral bands and n means the n th frequency component; $F(u)$ represents the frequency spectrum; $f(n)$ represents the discrete spectral signatures. It is worth noting that after we transform the spectral information into frequency domain, the distributions of the noise and useful

signal can be easily distinguished-noise is mainly distributed on high frequency part while useful signal is mainly distributed on low frequency part. Thus, we use a part of low frequency components to define the spectral similarity d_z :

$$d_z(i, k) = \text{SID}(\Phi_i^\alpha, \Phi_k^\alpha) \times \sin(\text{SAM}(\Phi_i^\alpha, \Phi_k^\alpha)) \quad (3)$$

in which Φ_i^α and Φ_k^α represent the low frequency components of pixel i and cluster centre \mathbf{R}_k ; the parameter α is defined to control the ratio of the frequency spectrum; SID is the acronym of the spectral information divergence, and SAM denotes the spectral angle mapper. The two widely spectral similarity measures are combined to enhance the discriminability of the proposed spectral similarity [Du, Chang, Ren et al. (2004)]. In the NRSS algorithm, the spatial similarity d_{xy} is defined by using Euclidean distance:

$$d_{xy}(i, k) = \sqrt{(x_i - x_k)^2 + (y_i - y_k)^2} \quad (4)$$

Combing the spectral similarity and spatial similarity, the new similarity $d(i, k)$ in NRSS can be formulated as:

$$d(i, k) = \sqrt{d_z(i, k)^2 + \lambda^2 (d_{xy}(i, k)/S)^2} \quad (5)$$

in which the parameter λ is defined to weigh the relative importance between the spectral similarity and spatial similarity. Based on the novel similarity measure, the assignment process is implemented in a $2S \times 2S$ region for each cluster center. Then, the mean vector of all the pixels belonging to the cluster is utilized for updating the new center. Finally, the assignment and updating steps are repeated until no pixel's label changes.

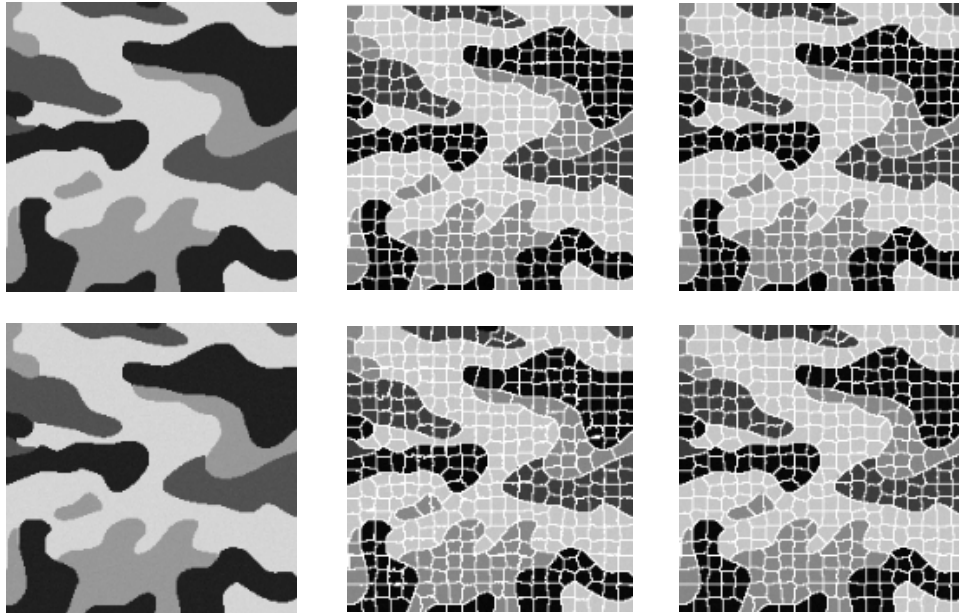
3 Experimental Results

In this experiment, the performance of the superpixel algorithms is evaluated on a synthetic HS image. First, 4 spectra are obtained from a real Pushbroom Hyperspectral Imager (PHI) [Zhang, Sun, Shang et al. (2016)] image. The all 124 spectral bands are utilized to generate the synthetic HS image. The spatial size of the synthetic HS image is 200×200 , where Fig. 1 shows the 50th band of the synthetic HS image.



Figure 1: The 50th spectral band of the synthetic hyperspectral image

In order to evaluate the noise robustness of the superpixel segmentation algorithms, random noise with different intensities is added to the synthetic HS image. In this experiment, the noise is assumed to be Gaussian distributed with zero mean and various variances. The indicator signal-to-noise ratio (SNR) is introduced to set the noise variance in each spectral band. In this experiment, we generate noisy synthetic HS images with SNR equals 15 dB, 20 dB, 25 dB, 30 dB, 35 dB, and 40 dB, respectively. For each noisy image, we apply the proposed NRSS and the widely used SLIC to segment the image into superpixels. In the proposed NRSS, we optimize the parameter $\alpha = 0.2$ and $\lambda = 10^{-3}$. Fig. 2 shows the superpixel segmentation results on synthetic images with various noise levels and different algorithms. From Fig. 2 we can see that with low noise levels, both of the NRSS and SLIC produce accurate superpixel segmentation results. However, the performance of the SLIC decreases rapidly with the increase of the noise levels, whereas the proposed NRSS is more insensitive to the noise. Moreover, the boundary adherence of superpixels generated by the two compared algorithms is quantitatively evaluated by using the measure boundary recall [Levinshtein, Stere, Kutulakos et al. (2009)]. Boundary recall measures the fraction of ground truth boundaries correctly recovered by the superpixel boundaries, where a high boundary recall value means that very few true image boundaries are missed. The values of boundary recall of the two compared algorithms are plotted in Fig. 3. In this figure, the black curve represents the boundary recall values of the proposed NRSS for images with various noise levels, and red curve denotes the corresponding results of SLIC. Experimental results shown in Fig. 3 further demonstrate that the NRSS is more robust to the noise.



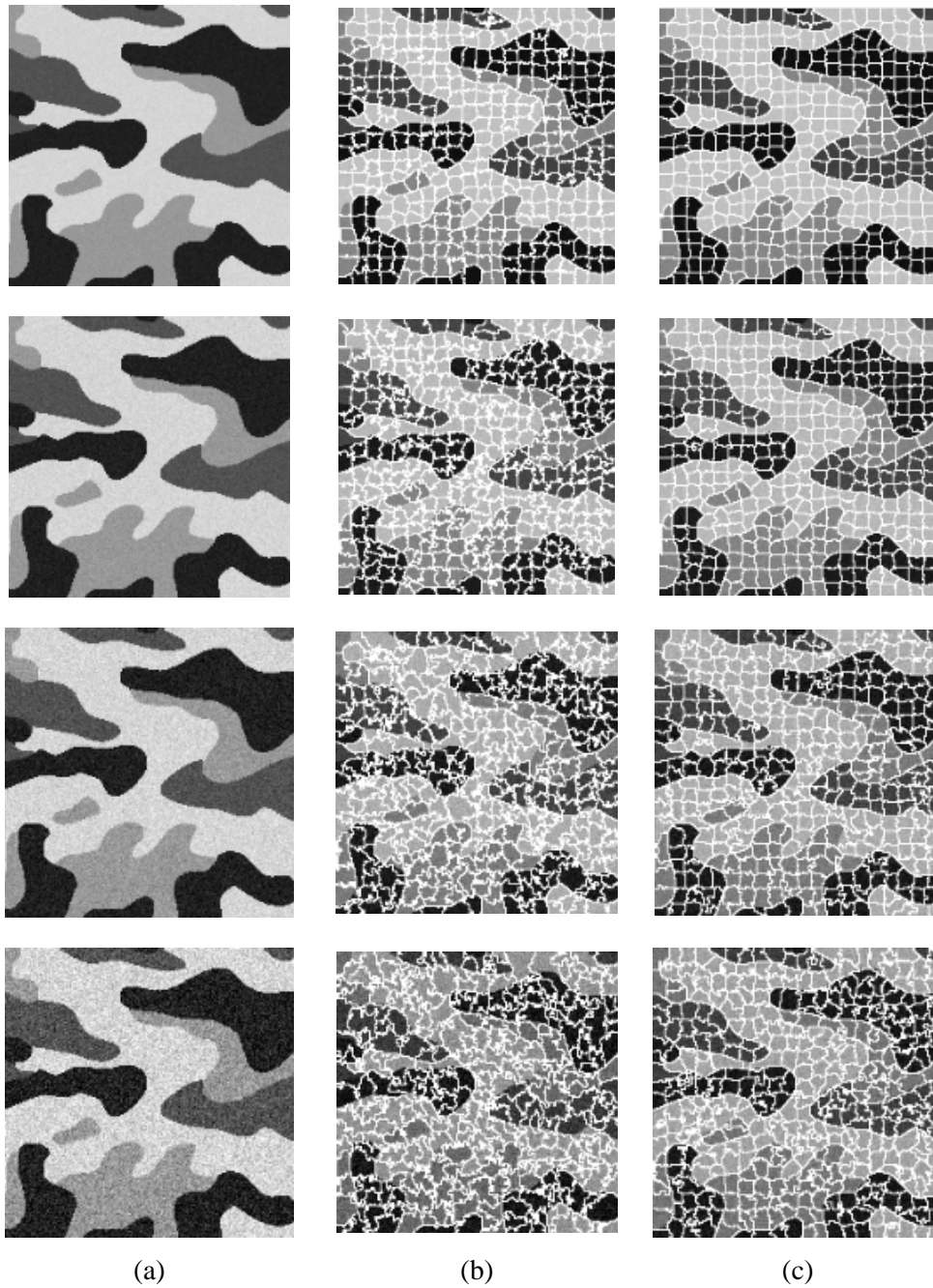


Figure 2: Column (a) exhibits the noisy synthetic hyperspectral images, where the SNR equals 40 dB, 35 dB, 30 dB, 25 dB, 20 dB, and 15 dB from row 1 to row 6, respectively; column (b) and (c) are the superpixel segmentation results with SLIC and NRSS, respectively

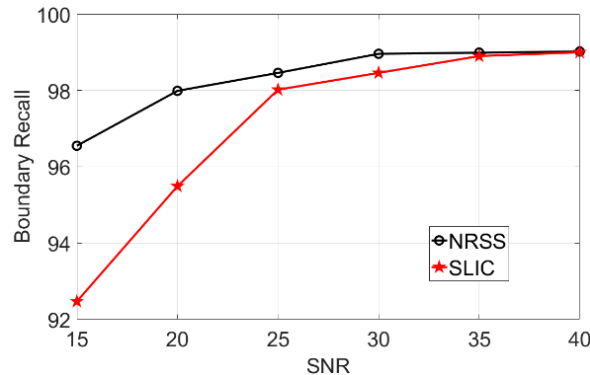


Figure 3: Boundary recall values of the superpixels generated by the NRSS and SLIC from the synthetic image with various SNR values

4 Conclusion

In this paper, we propose a noise-resistant superpixel segmentation algorithm for HS images. To make the generated superpixel more robust to noise, the spectral features are extracted in frequency domain, and a novel frequency-based spectral similarity measure is defined for the clustering of superpixels. Experimental results demonstrate that the proposed algorithm is robust to noise. However, the transformation process to frequency domain may increase the computation time. Speeding up the proposed superpixel segmentation algorithm without decreasing the accuracy will be investigated in further works.

Acknowledgement: This work was supported in part by the National Natural Science Foundation of China under Grant No. 61801222 and No. 61501522, and in part by the Project of Shandong Province Higher Educational Science and Technology Program under Grant No. KJ2018BAN047.

References

- Achanta, R.; Shaji, A.; Smith, K.; Lucchi, A.; Fua, P. et al.** (2012): SLIC superpixels compared to state-of-the-art superpixel methods. *IEEE Transactions on Pattern Analysis and Machine Intelligence*, vol. 34, no. 11, pp. 2274-2282.
- Du, Y.; Chang, C. I.; Ren, H.; Chang, C. C.; Jensen, J. O. et al.** (2004): New hyperspectral discrimination measure for spectral characterization. *Optical Engineering*, vol. 43, no. 8, pp. 1777-1787.
- Farag, A.; Lu, L.; Roth, H. R.; Liu, J.; Turkbey, E. et al.** (2017): A bottom-up approach for pancreas segmentation using cascaded superpixels and (deep) image patch labeling. *IEEE Transactions on Image Processing*, vol. 26, no. 1, pp. 386-399.
- He, L.; Ouyang, D.; Wang, M.; Bai, H.; Yang, Q. et al.** (2018): A method of identifying thunderstorm clouds in satellite cloud image based on clustering. *Computers, Materials & Continua*, vol. 57, no. 3, pp. 549-570.

- Levinshtein, A.; Stere, A.; Kutulakos, K. N.; Fleet, D. J.; Dickinson, S. J. et al.** (2009): Turbopixels: fast superpixels using geometric flows. *IEEE Transactions on Pattern Analysis and Machine Intelligence*, vol. 31, no. 12, pp. 2290-2297.
- Liu, Z.; Li, J.; Ye, L.; Sun, G.; Shen, L.** (2017): Saliency detection for unconstrained videos using superpixel-level graph and spatiotemporal propagation. *IEEE Transactions on Circuits and Systems for Video Technology*, vol. 27, no. 12, pp. 2527-2542.
- Liu, M. Y.; Tuzel, O.; Ramalingam, S.; Chellappa, R.** (2011): Entropy rate superpixel segmentation. *IEEE Conference on Computer Vision and Pattern Recognition*, pp. 2097-2104.
- Moore, A. P.; Prince, S. J.; Warrell, J.; Mohammed, U.; Jones, G.** (2008): Superpixel lattices. *IEEE Conference on Computer Vision and Pattern Recognition*, pp. 1-8.
- Shi, J.; Malik, J.** (2000): Normalized cuts and image segmentation. *IEEE Transactions on Pattern Analysis and Machine Intelligence*, vol. 22, no. 8, pp. 888-905.
- Vedaldi, A.; Soatto, S.** (2018): Quick shift and kernel methods for mode seeking. *European Conference on Computer Vision*, pp. 705-718.
- Vincent, L.; Soille, P.** (1991): Watersheds in digital spaces: an efficient algorithm based on immersion simulations. *IEEE Transactions on Pattern Analysis and Machine Intelligence*, no. 6, pp. 583-598.
- Wang, W.; Wang, C.; Liu, S.; Zhang, T.; Cao, X.** (2018): Robust target tracking by online random forests and superpixels. *IEEE Transactions on Circuits and Systems for Video Technology*, vol. 28, no. 7, pp. 1609-1622.
- Wei, X.; Yang, Q.; Gong, Y.; Ahuja, N.; Yang, M. H.** (2018): Superpixel hierarchy. *IEEE Transactions on Image Processing*, vol. 27, no. 10, pp. 4838-4849.
- Zhang, G.; Zheng, Y.; Xia, G.** (2018): Domain adaptive collaborative representation based classification. *Multimedia Tools and Applications*, pp. 1-22.
- Zhang, X.; Sun, Y.; Shang, K.; Zhang, L.; Wang, S.** (2016): Crop classification based on feature band set construction and object-oriented approach using hyperspectral images. *IEEE Journal of Selected Topics in Applied Earth Observations and Remote Sensing*, vol. 9, no. 9, pp. 4117-4128.